# Electrodeposition of nanowires for the detection of hydrogen gas

## Reginald M. Penner

Nanowires composed of noble metals are attractive candidates for chemical sensors because they are both ductile and chemically stable in air. The single application where electrodeposited metal nanowires have had the largest impact is that of hydrogen gas ($H_2$) sensing. The development of sensitive, selective, power-efficient, rapid-responding, and inexpensive $H_2$ sensors, for the purpose of detecting leaked $H_2$ in proximity to devices such as fuel cells, is an active area of research. In this application, a change in the dc electrical resistance of the nanowire from its background value signals the presence of $H_2$ and provides an estimate of its concentration. Two types of nanowires have been studied for use as hydrogen sensors: Electrodeposited nanowires composed of pure palladium metal (Pd) reversibly absorb hydrogen to form a hydride according to $Pd + xH_2 \rightarrow PdH_{2x}$. Alternatively, nanowires that transduce the presence of $H_2$ may be prepared by decorating an inert, electrically conductive support such as a carbon nanotube or a nickel nanowire with one or more eletrodeposited palladium nanoparticles. These palladium nanoparticles impart selectivity to $H_2$ and cause the electrical conductivity of the composite particle/support to be modulated in the presence of $H_2$. Here we summarize recent contributions of electrodeposition to the development of nanowire-based sensors for $H_2$.

## Introduction

Chemical sensing using nanowires almost always means *semiconductor* nanowires. Lieber and co-workers were the first to demonstrate in 2001[1] that chemically modified single crystalline silicon nanowires could function as ChemFETs[2,3]—transistors in which the gating of the channel conductivity is effected by the specific binding of ions to receptors (e.g., antibodies) present at the surface of the nanowire.[4–6]

Since a pioneering study of $SnO_2$ nanobelts by Wang and co-workers in 2002,[7] semiconducting nanowires composed of metal oxides, especially tin oxide ($SnO_2$), have been extensively used as gas sensors.[8–19] Although more than one mechanism has been proposed to account for the sensing properties of these nanowires, in one case, a redox reaction of a reactive gas such as $SO_2$, $H_2$, or $NH_3$ with the $SnO_2$ surface or dopant atoms present at the surface alters the electrical conductivity of the nanowire.

Nanowires composed of noble metals are attractive candidates for chemical sensors because they are both ductile and chemically stable in air. The single application where electrodeposited metal nanowires have had the largest impact is that of hydrogen gas sensing. The development of sensitive, selective, power-efficient, rapid-responding, and inexpensive

hydrogen gas sensors continues to be an active area of research. Hydrogen gas is odorless and flammable above 4% in air, so $H_2$ sensors must be deployed in proximity to devices that employ $H_2$ as a fuel, such as within fuel cell-powered automobiles, mobile electronics, and stationary power sources.[20] $H_2$ safety sensors based upon palladium (Pd) resistors have been known since the pioneering work of Hughes and Schubert in 1992.[21] Those workers prepared resistors using evaporated films of Pd-Ni (8–20 vol%) with thicknesses in the 50 nm range. Those devices produced response times of $\approx 10$ s at 4% $H_2$ and $\approx 20$ s at 1% $H_2$ while achieving a limit-of-detection ($LOD_{H_2}$) below 0.1%.[21] A Pd-Ni thin-film resistor achieves many design objectives for hydrogen safety sensors, including a low manufacturing cost, high sensitivity and accuracy, good stability, and a simple, rugged design, but its response times (10–20 s) are too slow by approximately an order of magnitude relative to targets set by the Department of Energy for this technology.[22]

Resistive sensors based upon Pd nanowires retain the simplicity of Hughes' palladium film resistors while offering the possibility for accelerated sensor response and recovery and extremely low power consumption. In this review, we summarize recent efforts to employ electrodeposited nanowires, or components

Reginald M. Penner, University of California, Irvine, CA 92697, USA, rmpenner@uci.edu

of nanowires, as $H_2$ sensors, and we highlight a new fabrication method for synthesizing palladium nanowires that streamlines the fabrication of hydrogen sensors based upon single, polycrystalline Pd nanowires.

## Electrodeposition by electrophoresis of single Pd nanowires between shaped electrodes

Myung and co-workers[23] demonstrated a versatile concept for fabricating single Pd nanowires for $H_2$ sensors in 2004. They showed that single palladium (Pd) nanowires, 200–500 nm in width, could be electrodeposited galvanostatically between lithographically patterned gold electrodes with 2.5 μm spacing on a glass surface. The application of a controlled current of 100 nA between these two electrodes in an aqueous solution containing $Pd^{2+}$ induced the nucleation of a Pd nanowire at one of these electrodes and the growth of the nanowire in the direction of the second electrode across this gap.[23] Nanowires with minimum widths in the 70 nm range were obtained using this approach, and low-resistance contacts between the gold electrodes and the nanowire also were achieved in this work.[23]
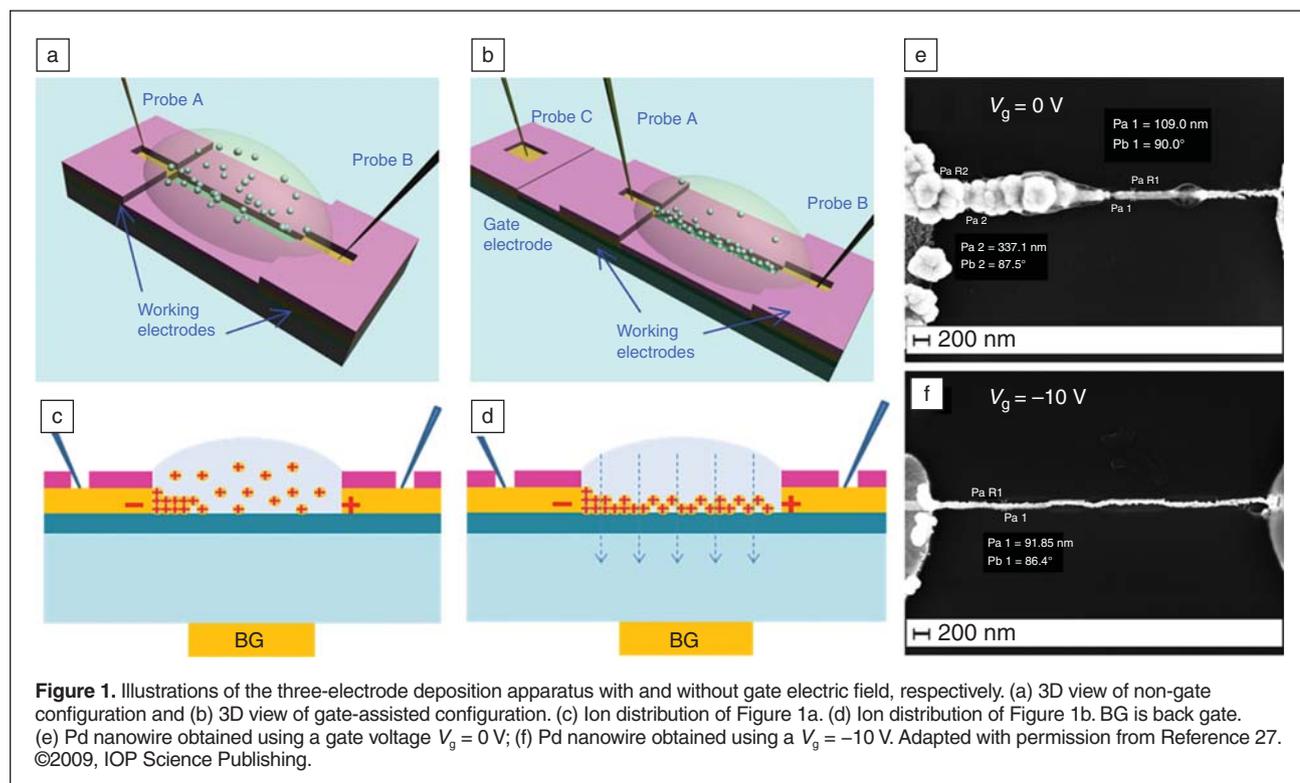
Yun and co-workers[24,25] characterized the properties of the Pd nanowires produced by this process for the detection of $H_2$. Once the circuit between the two electrodes was completed by nanowire growth across the 2–7 μm gap, the electrolyte solution was removed, and the resistance of the nanowire was monitored as it was exposed to $H_2$.[24,25] In these early experiments, nanowires with widths between 70 and 300 nm showed detectable resistance increases upon exposure to $H_2$ at concentrations ranging from 200 ppm to 10%.[24,25]

With optimization of this "electrophoresis" nanowire growth process, Yun and co-workers[26] have obtained a higher degree of width uniformity for the deposited Pd nanowires, culminating the ability to produce smaller wires with widths down to 30 nm. A recent innovation in the nanowire growth process[27] has been the addition of a third electrical contact to this apparatus (**Figure 1a–d**).[27] This third contact is obtained by patterning the two gold electrodes on a silicon wafer covered with a thin gate oxide. The application of a −10 V gate voltage to the silicon back gate during nanowire electrodeposition modifies the morphology of the nascent nanowire during growth, producing a higher degree of wire width uniformity and the possibility to reproducibly obtain nanowires with diameters less than 50 nm (Figure 1e–f). The $H_2$ sensing properties of these nanowires, however, have not yet been reported.[27]

Zamborini et al.[40] showed that the directionality of palladium growth between electrodes can be controlled by functionalizing an electrode with a conductive polymer. The nucleation of palladium then occurs preferentially on the other electrode, and Pd dendrites are obtained that cross a 5 μm gap. The $H_2$ sensors derived from these nanostructures show a reversible increase in resistance upon exposure to $H_2$, with a rapid time response of <60 s and a $LOD_{H_2}$ of 0.11%.

## Electrodeposition of Pd nanoparticles onto carbon nanotubes

Dai and co-workers[28] were the first to create hydrogen gas sensors by modifying electronically conductive but $H_2$-unreactive



**Figure 1.** Illustrations of the three-electrode deposition apparatus with and without gate electric field, respectively. (a) 3D view of non-gate configuration and (b) 3D view of gate-assisted configuration. (c) Ion distribution of Figure 1a. (d) Ion distribution of Figure 1b. BG is back gate. (e) Pd nanowire obtained using a gate voltage $V_g = 0$ V; (f) Pd nanowire obtained using a $V_g = −10$ V. Adapted with permission from Reference 27. ©2009, IOP Science Publishing.
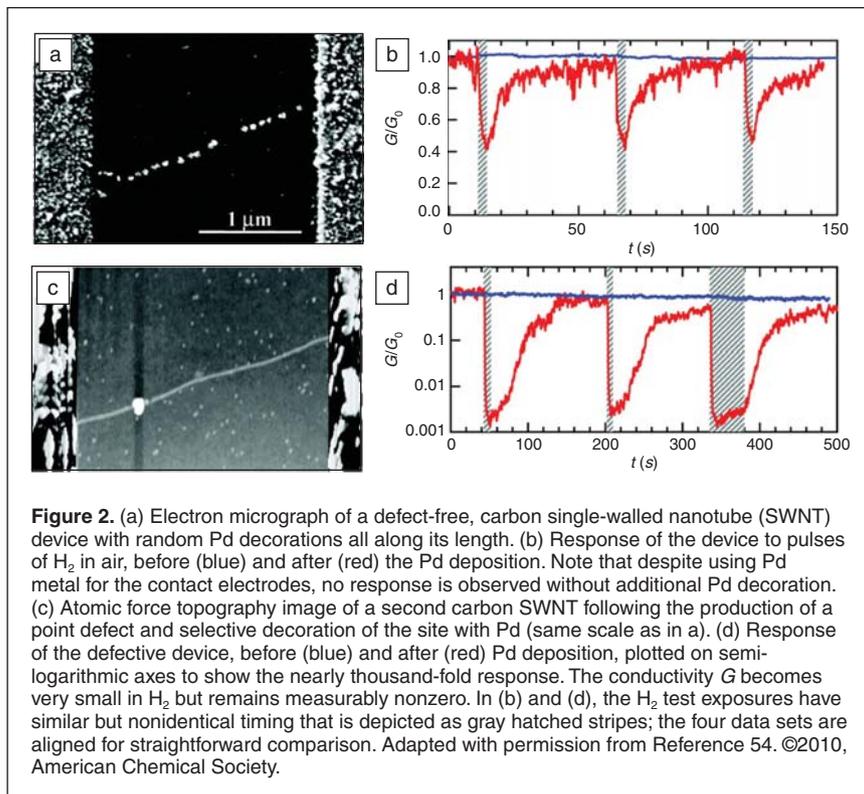
carbon nanotubes with evaporated palladium metal in 2001. In their experiment, 5Å of Pd was evaporated onto one carbon single-walled nanotube (SWNT). This decorated nanotube showed a $LOD_{H_2}$ of 4 ppm, a response time of $\approx$15 s, and a recovery time of 50–200 s, depending on $H_2$ concentration.[28] Since then, the concept of using the electrodeposition of Pd instead of evaporation to decorate nanotubes has been explored in some detail.[29–36] Myung and co-workers[36] showed in 2007 that films of carbon nanotubes, decorated with electrodeposited Pd particles, produced an increased resistance ($\Delta R/R_0 \approx 0.42\%$/ppm) upon exposure to $H_2$ characterized by a $LOD_{H_2}$ of 100 ppm; however, the response time for these devices exceeded 10 minutes.[36] Sun and Wang[32,33] also investigated the potential of carbon nanotube mats decorated by electrodeposited Pd particles, and these workers created $H_2$ sensors on flexible polyethylene terephthalate substrates characterized by an $LOD_{H_2}$ of 100 ppm, with somewhat more rapid response times to $H_2$ of a few minutes.

The mechanism by which the palladium particles communicate electrically with carbon nanotubes is not well understood. Collins and co-workers[37] have demonstrated that the presence of defects in the carbon nanotube increases the electronic coupling that occurs between the Pd particle and the nanotube. The defects within the SWNT can be electrochemically generated,[38,39] and the subsequent nucleation and growth of electrodeposited Pd on such a defective SWNT occurs with a high degree of selectivity at the defect site(s).[37] SWNTs with induced defects on which Pd has been electrodeposited (**Figure 2b and 2d**) show a decreased conductivity $G/G_0$ (same as increased resistance) in the presence of $H_2$ that is higher by three orders of magnitude as compared with the response observed at pristine, defect-free SWNTs decorated with electrodeposited Pd, in spite of the fact that a much larger quantity of Pd decorates the SWNT in this case (Figure 2a and 2c).[37]

Nanowires of metals other than Pd also can serve as inert supports in much the same way as carbon SWNTs. For example, Myung and co-workers[34] recently showed that nickel nanowires could be controllably broken to produce a gap 100 nm in width. This gap could then be backfilled with Pd by electrodeposition. The resulting hybrid Ni/Pd structure functioned as a hydrogen sensor over the concentration range from 0.1% to 4% $H_2$.[34]

## Lithographically patterned nanowire electrodeposition

We first investigated the properties of ensembles of Pd nanowires for detecting hydrogen gas ($H_2$) in 2001.[41] These nanowires spontaneously fractured upon exposure to $H_2$ above 1–2%,



**Figure 2.** (a) Electron micrograph of a defect-free, carbon single-walled nanotube (SWNT) device with random Pd decorations all along its length. (b) Response of the device to pulses of $H_2$ in air, before (blue) and after (red) the Pd deposition. Note that despite using Pd metal for the contact electrodes, no response is observed without additional Pd decoration. (c) Atomic force topography image of a second carbon SWNT following the production of a point defect and selective decoration of the site with Pd (same scale as in a). (d) Response of the defective device, before (blue) and after (red) Pd deposition, plotted on semi-logarithmic axes to show the nearly thousand-fold response. The conductivity $G$ becomes very small in $H_2$ but remains measurably nonzero. In (b) and (d), the $H_2$ test exposures have similar but nonidentical timing that is depicted as gray hatched stripes; the four data sets are aligned for straightforward comparison. Adapted with permission from Reference 54. ©2010, American Chemical Society.

and this fracturing process activated a unique mechanism for sensor function that permitted the fractured nanowires to detect $H_2$ at concentrations above 2%.[41,42] The Pd nanowires investigated in these experiments were prepared by electrodepositing these metals onto stepped graphite electrodes.[43,44] This process, called electrochemical step edge decoration (ESED), produced ensembles of hundreds or thousands of metal nanowires oriented in parallel arrays that were spaced on the graphite surface by less than one micron. We were able to fabricate sensors from ensembles of metal nanowires, but single nanowires could not be electrically isolated from these ensembles, and sensors containing single metal nanowires were not realized.

These deficiencies of the ESED process motivated the development of a new nanowire fabrication method with the capability to pattern metal nanowires on dielectrics in a parallel process. Erik Menke, a graduate student, developed the process in 2005. Menke demonstrated that photolithography could be used to prepare a template for electrodeposition of gold nanowires.[45] This template consisted of an evaporated nickel layer covered by photoresist that was photopatterned. The exposed nickel was subsequently removed by oxidative dissolution, and these etching conditions were optimized to controllably over-etch the nickel layer, producing an undercut of the photoresist at the edges of the patterned region (**Figure 3**). This template was then immersed in a gold plating solution from which gold was electrodeposited at the nickel nanoband electrode. After removal of the photoresist and nickel, scanning electron microscopy (SEM) images of the resulting nanowires showed they were rectangular in cross-section, an indication that their dimensions had been determined by the

horizontal trench in which they nucleated and grew. We named this new method lithographically patterned nanowire electrodeposition or LPNE.[45–47] LPNE shares the ability of electron beam lithography (EBL) to pattern metal nanowires that are much smaller than the diffraction limit of light, ≈λ/2 (where λ is the wavelength), but like photolithography, LPNE is a parallel process that can be used to blanket the surface of a silicon wafer with nanowires in a single series of processing steps.[45–47] LPNE also can be used to prepare a single nanowire in isolation on a surface, a capability that often is exploited.

The growth by electrodeposition of a Pd nanowire in the horizontal trench produced in the LPNE process occurs in three phases (**Figure 4**).[45] First, immediately after the application of a plating voltage for palladium, the current increases as palladium nucleates along the entire length of the nickel nanoband. When this nucleation process is complete, a quasi-constant deposition current is observed during growth of the confined metal nanowires, because the wetted surface area of the confined wire is constant, and because for such a kinetically controlled reaction, the deposition current per unit area of the metal is constant. Terminating growth during this phase results in a nanowire having a rectangular cross section, such as seen in Figure 4b. If wire growth is continued, deposited metal fills the trench and begins to emerge from it, and the total current increases because the wetted surface area increases. This "blooming" or "overgrowth" of the nanowire is generally avoided because with it, one relinquishes control over the thickness of the nanowire along one of its edges. However, intentionally allowing a nanowire to bloom provides a convenient means by which the trench depth may be determined, since the deposited nanowire is an imprint of the trench, and its dimensions may be determined directly from the bloomed nanowire using SEM (Figure 4c).

SEM images of typical nanowires (**Figure 5**) show the degree of uniformity that is obtained for nanowires of gold and palladium. The LPNE method provides for orthogonal control of nanowire width and thickness: The thickness dimension is controlled by the thickness of the nickel layer deposited in the first step of the process (**Figure 6a**), whereas the width dimension depends on the electrodeposition duration (Figure 6b). Because they are controlled by completely different process parameters, these two crit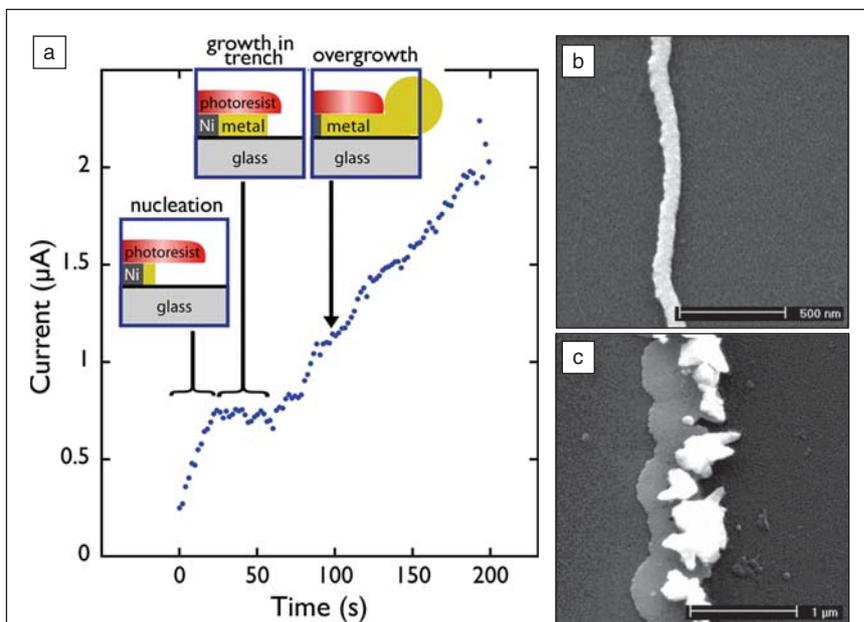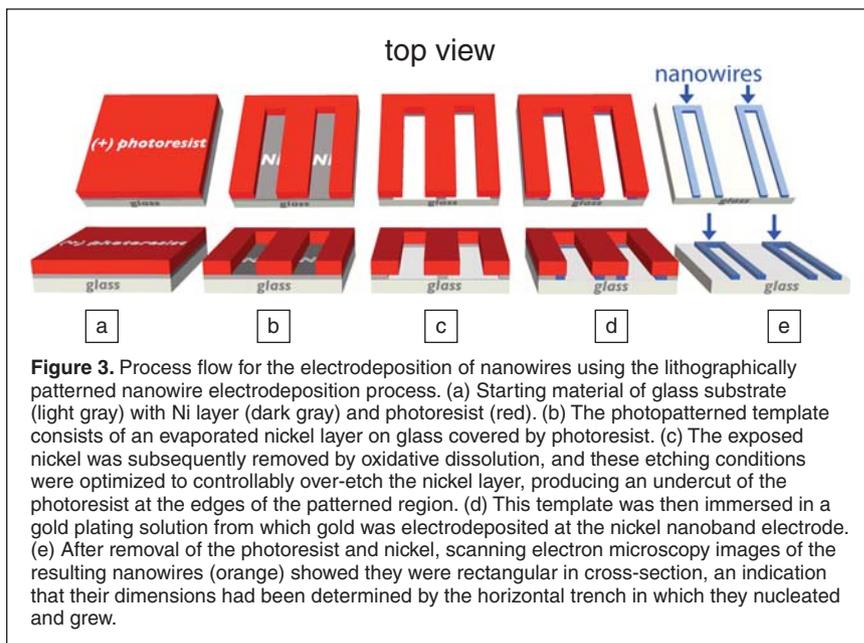ical nanowire dimensions can be changed independently and without cross-talk. Minimum widths for gold and palladium nanowires are 20–30 nm, while the minimum thickness is ≈5 nm. The rectangular cross-section of these nanowires is apparent in the atomic



**Figure 3.** Process flow for the electrodeposition of nanowires using the lithographically patterned nanowire electrodeposition process. (a) Starting material of glass substrate (light gray) with Ni layer (dark gray) and photoresist (red). (b) The photopatterned template consists of an evaporated nickel layer on glass covered by photoresist. (c) The exposed nickel was subsequently removed by oxidative dissolution, and these etching conditions were optimized to controllably over-etch the nickel layer, producing an undercut of the photoresist at the edges of the patterned region. (d) This template was then immersed in a gold plating solution from which gold was electrodeposited at the nickel nanoband electrode. (e) After removal of the photoresist and nickel, scanning electron microscopy images of the resulting nanowires (orange) showed they were rectangular in cross-section, an indication that their dimensions had been determined by the horizontal trench in which they nucleated and grew.



**Figure 4.** The filling and the eventual over-filling of the trench with gold, platinum, or palladium produces a distinctive wire electrodeposition current transient: (a) Electrodeposition current versus time for the potentiostatic nucleation, growth, and overgrowth (or "blooming"), of a palladium nanowire at +0.225 V versus standard calomel electrode. This aqueous solution contained 2 mM Pd(NO₃)₂, 2 mM saccharine, and 0.1 M KCl. The quasi-constant current seen from 20 to 50 seconds occurs because for this kinetically controlled deposition process, current is proportional to the wetted surface area, which remains constant while growth of the nanowire is confined to the horizontal trench. (b) Gold nanowire with a rectangular cross-section obtained for trench-confined growth for 100 s and (c) gold nanowire deposited for 1000 s showing "blooming" from the edge of the photoresist. Adapted with permission from Reference 55. ©2006, Nature Publishing Group.

**Figure 5.** Scanning electron micrographs of linear nanowires: (a) gold and (b) palladium. Adapted with permission from Reference 46. ©2008, American Chemical Society.



**Figure 6.** Control of nanowire thickness and width for wires of Au, Pt, Pd, and Bi: (a) Nanowire thickness measured by atomic force microscopy versus the thickness of the nickel or silver sacrificial layer. (b) Nanowire width measured by scanning electron microscopy versus the electrodeposition duration. (c) Nanowire cross-sectional profiles measured by atomic force microscopy. Adapted with permission from Reference 46. ©2008, American Chemical Society.

force microscope traces of gold nanowires (Figure 6c). Metal nanowires prepared by LPNE are polycrystalline with grain sizes typically in the 4–100 nm range.

In the LPNE process, electrodeposition produces nanowires, so many materials can be used to make nanowires using this method. In addition to Pd, to date we have used LPNE to prepare nanowires composed of other metals (e.g., Au, Pt, Pd),[45–47] a semimetal (e.g., bismuth),[46] a II–VI semiconductor (CdSe), and a thermoelectric material (PbTe).[48,49]

## Palladium nanowire-based H$_2$ sensors prepared by LPNE

Our early work on the use of Pd nanowires for H$_2$ detection revealed a serious problem:[41,42,50–52] Exposure of these nanowires to H$_2$ above 1–2% induced periodic fracturing of the nanowire along its axis. Fracturing was observed to occur for Pd nanowires in the 200–300 nm diameter range prepared by electrochemical step edge decoration[41,42] and also for the smaller Pd nanowires prepared by LPNE.[52] Although fractured nanowires retain the ability to detect H$_2$ at concentrations higher than 1–2%,[41,42,52] this limit-of-detection is much too high to enable the use of these devices as safety sensors. We experimented with the addition of ethylenediaminetetraacetic acid (EDTA)—a complexing agent for Pd$^{2+}$—to the plating solution used for nanowire growth. The Pd nanowires prepared from EDTA-containing solutions appeared identical to those prepared in its absence (**Figure 7a–b**), but the presence of EDTA in the plating solution increased the mean grain diameter of the nanowire from 6 nm to 15 nm (Figure 7 c–d). Remarkably, this subtle change eliminates fracture as a failure mode for these nanowires in the presence of H$_2$ at any concentration.[52]

The performance of two Pd nanowire sensors prepared using this procedure is summarized in **Figure 8**. These nanowires are able to detect H$_2$ at concentrations ranging from 2 ppm to 10%—reducing the limit-of-detection by a factor of 1/50,000 as compared with fractured Pd nanowires.[41,42,52] A critical issue for H$_2$ sensors tasked with detecting leaked H$_2$ is the response time, defined as the time required for the resistance of the sensor to increase from 10% to 90% of the final resistance value at each concentration. A strategy employed to accelerate the response of resistor-based H$_2$ sensors has been to resistively heat the sensor surface, but even when carried out with elegant engineering,[53] this approach compromises the power efficiency of the device. In our initial investigations of single Pd nanowire devices operated at room temperature without joule heating, we have measured response times in the range from 2 s (at 10% H$_2$) to 500 s (at 2 ppm) for a sensor containing a 11 × 93 nm nanowire. Since the lower explosion limit for H$_2$ is 4%, a response at 1% H$_2$ is considered a critical metric, and the U.S. Department of Energy has suggested a target of 60 s for sensor response at this concentration. For three nanowires ranging from 10 nm to 48 nm in thickness, we measured response times ranging from 20 s to 70 s at 1% H$_2$. Both response times and recovery times are observed to decrease with a reduction in the nanowire dimensions—both width and thickness. But significantly, no penalty attends the use
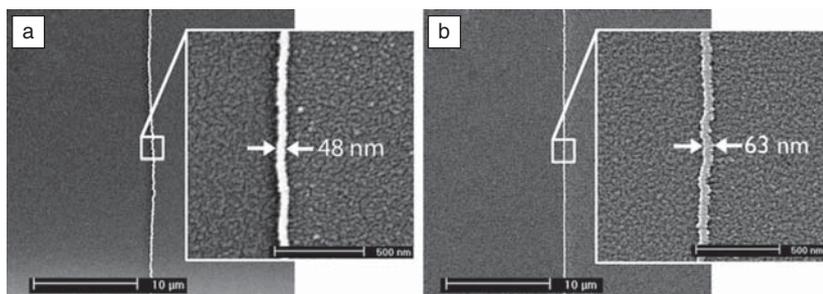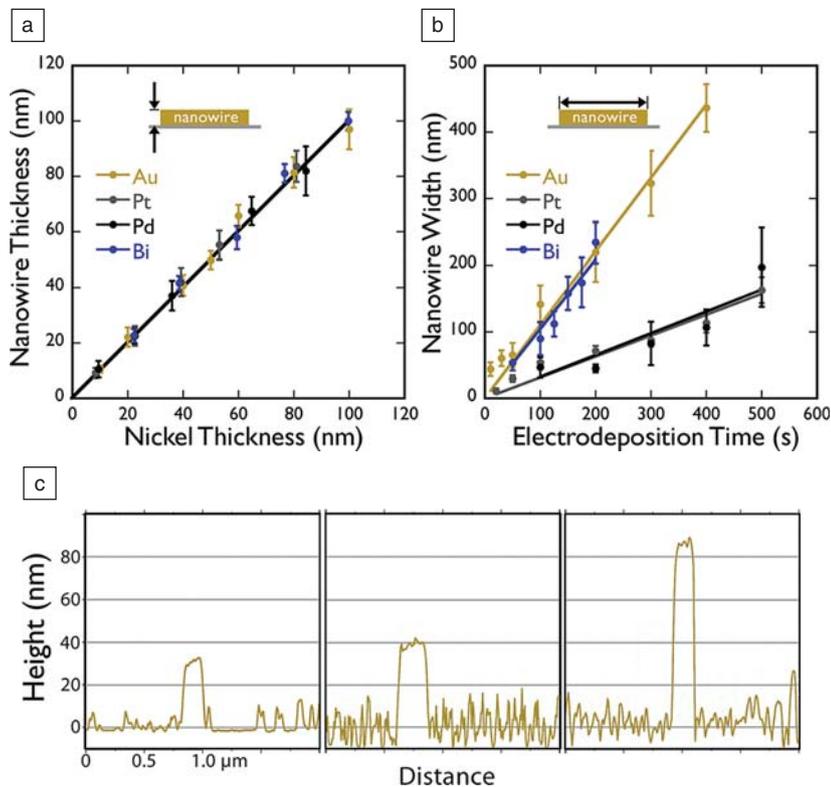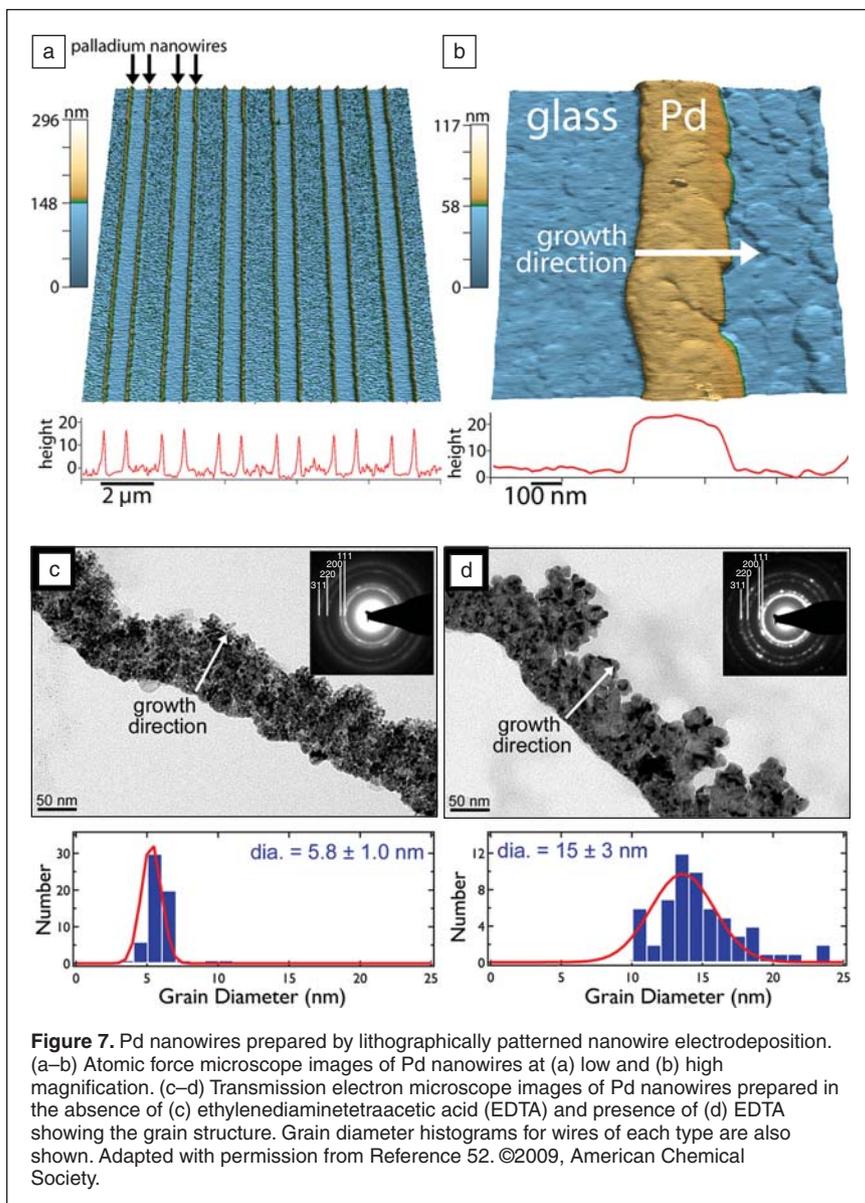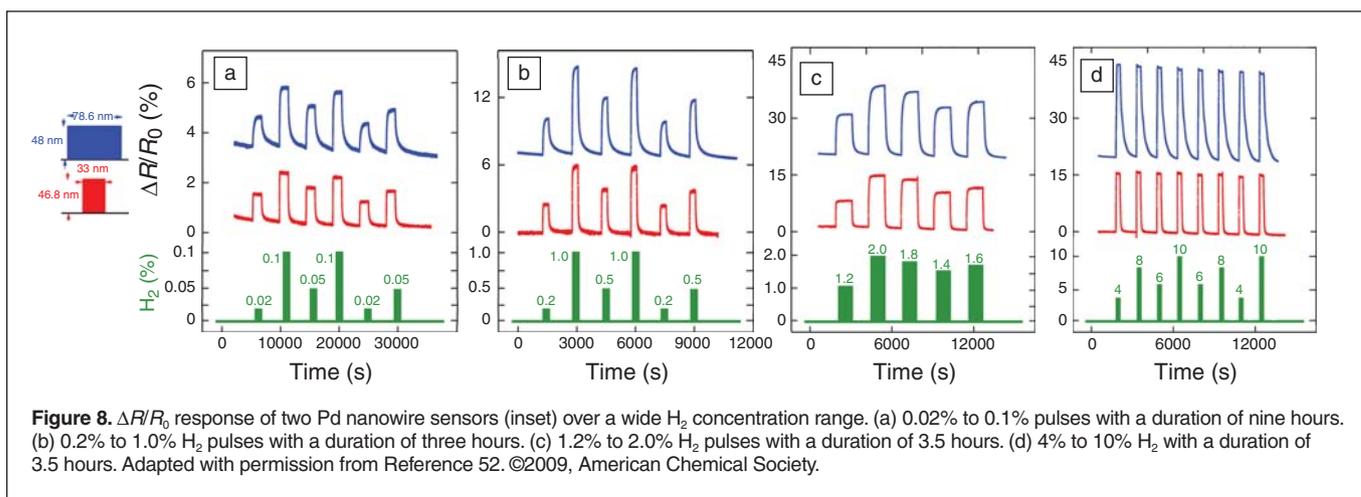
**Figure 7.** Pd nanowires prepared by lithographically patterned nanowire electrodeposition. (a–b) Atomic force microscope images of Pd nanowires at (a) low and (b) high magnification. (c–d) Transmission electron microscope images of Pd nanowires prepared in the absence of (c) ethylenediaminetetraacetic acid (EDTA) and presence of (d) EDTA showing the grain structure. Grain diameter histograms for wires of each type are also shown. Adapted with permission from Reference 52. ©2009, American Chemical Society.

of the smallest nanowires we have investigated in terms of the durability of these wires or the reliability of the single nanowire $H_2$ sensors constructed from them. These smallest wires exhibit the highest $H_2$ sensing performance in terms of sensitivity and response/recovery time.

## Summary

Three distinct approaches for preparing $H_2$-sensitive nanowires for sensors have been described to date. In all three cases, fundamental aspects of the sensing mechanism responsible for signal transduction by the palladium, sensitivity to $H_2$, and the measured response and recovery times remain to be elucidated. With this information, an optimization of these sensors will be possible, and the performance of these devices can be further improved. But it is already clear that electrodeposition has found an important niche for the versatile fabrication of nanowires for $H_2$ sensors that are capable of state-of-the-art $H_2$ sensing performance.

## Acknowledgments

**Figure 8.** $\Delta R/R_0$ response of two Pd nanowire sensors (inset) over a wide $H_2$ concentration range. (a) 0.02% to 0.1% pulses with a duration of nine hours. (b) 0.2% to 1.0% $H_2$ pulses with a duration of three hours. (c) 1.2% to 2.0% $H_2$ pulses with a duration of 3.5 hours. (d) 4% to 10% $H_2$ with a duration of 3.5 hours. Adapted with permission from Reference 52. ©2009, American Chemical Society.

## References

1. Y. Cui, Q.Q. Wei, H.K. Park, C.M. Lieber, *Science* **293**, 1289 (2001).
2. D.N. Reinhoudt, *Sens. Actuators, B* **24**, 197 (1995).
3. D.N. Reinhoudt, J.F.J. Engbersen, Z. Brzozka, H.H. Vandenvlekkert, G.W.N. Honig, H.A.J. Holterman, U.H. Verkerk, *Anal. Chem.* **66**, 3618 (1994).
4. F. Patolsky, G.F. Zheng, C.M. Lieber, *Nat. Protoc.* **1**, 1711 (2006).
5. W.U. Wang, C. Chen, K.H. Lin, Y. Fang, C.M. Lieber, *Proc. Natl. Acad. Sci. U.S.A.* **102**, 3208 (2005).
6. F. Patolsky, G.F. Zheng, O. Hayden, M. Lakadamyali, X.W. Zhuang, C.M. Lieber, *Proc. Natl. Acad. Sci. U.S.A.* **101**, 14017 (2004).
7. E. Comini, G. Faglia, G. Sberveglieri, Z.W. Pan, Z.L. Wang, *Appl. Phys. Lett.* **81**, 1869 (2002).
8. F. Hernandez-Ramirez, J.D. Prades, A. Tarancon, S. Barth, O. Casals, R. Jimenez-Diaz, E. Pellicer, J. Rodriguez, M.A. Juli, A. Romano-Rodriguez, J.R. Morante, S. Mathur, A. Helwig, J. Spannhake, G. Mueller, *Nanotechnol.* **18** (2007).
9. F. Hernandez-Ramirez, A. Tarancon, O. Casals, J. Arbiol, A. Romano-Rodriguez, J.R. Morante, *Sens. Actuators, B* **121**, 3 (2007).
10. N.D. Hoa, N.V. Quy, D. Kim, *Sens. Actuators, B* **142**, 253 (2009).
11. H. Huang, Y.C. Lee, O.K. Tan, W. Zhou, N. Peng, Q. Zhang, *Nanotechnol.* **20** (2009).
12. A. Kolmakov, Y.X. Zhang, G.S. Cheng, M. Moskovits, *Adv. Mater.* **15**, 997 (2003).
13. A. Kolmakov, Y.X. Zhang, M. Moskovits, *Nano Lett.* **3**, 1125 (2003).
14. Y. Shen, T. Yamazaki, Z.F. Liu, D. Meng, T. Kikuta, *J. Alloys Compd.* **488**, L21 (2009).
15. Y.B. Shen, T. Yamazaki, Z.F. Liu, D. Meng, T. Kikuta, N. Nakatani, M. Saito, M. Mori, *Sens. Actuators, B* **135**, 524 (2009).
16. V.V. Sysoev, J. Goschnick, T. Schneider, E. Strelcov, A. Kolmakov, *Nano Lett.* **7**, 3182 (2007).
17. V.V. Sysoev, T. Schneider, J. Goschnick, I. Kiselev, W. Habicht, H. Hahn, E. Strelcov, A. Kolmakov, *Sens. Actuators, B* **139**, 699 (2009).
18. L.C. Tien, D.P. Norton, B.P. Gila, S.J. Pearton, H.T. Wang, B.S. Kang, F. Ren, *Appl. Surf. Sci.* **253**, 4748 (2007).
19. Q. Wan, J. Huang, Z. Xie, T.H. Wang, E.N. Dattoli, W. Lu, *Appl. Phys. Lett.* **92** (2008).
20. L.A. Lewis, *The Palladium Hydrogen System* (Academic Press, London, 1967).
21. R.C. Hughes, W.K. Schubert, *J. Appl. Phys.* **71**, 542 (1992).
22. The Department of Energy, Vol. Funding Opportunity Announcement: DE-PS36-09G099004 (The Department of Energy: Golden, CO, 2009).
23. M.A. Bangar, K. Ramanathan, M. Yun, C. Lee, C. Hangarter, N.V. Myung, *Chem. Mater.* **16**, 4955 (2004).
24. Y. Im, C. Lee, R.P. Vasquez, M.A. Bangar, N.V. Myung, E.J. Menke, R.M. Penner, M.H. Yun, *Small* **2**, 356 (2006).
25. M.H. Yun, N.V. Myung, R.P. Vasquez, C.S. Lee, E. Menke, R.M. Penner, *Nano Lett.* **4**, 419 (2004).
26. Y.S. Hu, D. Perello, U. Mushtaq, M.H. Yun, *IEEE Trans. Nanotechnol.* **7**, 693 (2008).
27. Y. Hu, A.C. To, M. Yun, *Nanotechnology* **20** (2009).
28. J. Kong, M.G. Chapline, H.J. Dai, *Adv. Mater.* **13**, 1384 (2001).
29. D.R. Kauffman, D.C. Sorescu, D.P. Schofield, B.L. Allen, K.D. Jordan, A. Star, *Nano Lett.* **10**, 958 (2010).
30. B.L. Allen, P.D. Kichambare, A. Star, *ACS Nano* **2**, 1914 (2008).
31. D.R. Kauffman, A. Star, *Angew. Chem. Int. Ed.* **47**, 6550 (2008).
32. Y.G. Sun, H.H. Wang, *Adv. Mater.* **19**, 2818 (2007).
33. Y.G. Sun, H.H. Wang, *Appl. Phys. Lett.* **90** (2007).
34. S. Mubeen, B. Yoo, N.V. Myung, *Appl. Phys. Lett.* **93**, (2008).
35. T. Zhang, S. Mubeen, N.V. Myung, M.A. Deshusses, *Nanotechnol.* **19** (2008).
36. S. Mubeen, T. Zhang, B. Yoo, M.A. Deshusses, N.V. Myung, *J. Phys. Chem. C* **111**, 6321 (2007).
37. V.R. Khalap, T. Sheps, A.A. Kane, P.G. Collins, *Nano Lett.* **10**, 896 (2010).
38. Y. Kanai, V.R. Khalap, P.G. Collins, J.C. Grossman, *Phys. Rev. Lett.* **104** (2010).
39. B.R. Goldsmith, J.G. Coroneus, A.A. Kane, G.A. Weiss, P.G. Collins, *Nano Lett.* **8**, 189 (2008).
40. R. Dasari, F.P. Zamborini, *J. Am. Chem. Soc.* **130**, 16138 (2008).
41. F. Favier, E.C. Walter, M.P. Zach, T. Benter, R.M. Penner, *Science* **293**, 2227 (2001).
42. E.C. Walter, F. Favier, R.M. Penner, *Anal. Chem.* **74**, 1546 (2002).
43. E.C. Walter, B.J. Murray, F. Favier, G. Kaltenpoth, M. Grunze, R.M. Penner, *J. Phys. Chem. B* **106**, 11407 (2002).
44. E.C. Walter, M.P. Zach, F. Favier, B.J. Murray, K. Inazu, J.C. Hemminger, R.M. Penner, *ChemPhysChem* **4**, 131 (2003).
45. E.J. Menke, M.A. Thompson, C. Xiang, L.C. Yang, R.M. Penner, *Nat. Mater.* **5**, 914 (2006).
46. C.X. Xiang, S.C. Kung, D.K. Taggart, F. Yang, M.A. Thompson, A.G. Guell, Y.A. Yang, R.M. Penner, *ACS Nano* **2**, 1939 (2008).
47. C.X. Xiang, Y.G. Yang, R.M. Penner, *Chem. Commun.* 859 (2009).
48. Y. Yang, S.C. Kung, D.K. Taggart, C. Xiang, F. Yang, M.A. Brown, A.G. Guell, T.J. Kruse, J.C. Hemminger, R.M. Penner, *Nano Lett.* **8**, 2447 (2008).
49. Y. Yang, D. Taggart, M.A. Brown, F. Yang, J.C. Hemminger, R.M. Penner, *ACS Nano* **3**, 4144 (2010).
50. E.C. Walter, K. Ng, M.P. Zach, R.M. Penner, F. Favier, *Microelectron. Eng.* **61–2**, 555 (2002).
51. E.C. Walter, R.M. Penner, H. Liu, K.H. Ng, M.P. Zach, F. Favier, *Surf. Interface Anal.* **34**, 409 (2002).
52. F. Yang, D.K. Taggart, R.M. Penner, *Nano Lett.* **9**, 2177 (2009).
53. F. Dimeo, I.S. Chen, P. Chen, J. Neuner, A. Roerhl, J. Welch, *Sens. Actuators, B* **117**, 10 (2006).
54. V.R. Khalap, T. Sheps, A.A. Kane, P.G. Collins, *Nano Lett.* **10**, 896 (2010).
55. E. Menke, M.A. Thompson, C. Xiang, L.C. Yang, R.M. Penner, *Nat. Mater.* **5**, 914 (2006). ☐